

# Theoretical Optimal Trajectories for Reducing the Environmental Impact of Commercial Aircraft Operations

Cesar Celis<sup>1</sup>, Vishal Sethi<sup>2</sup>, David Zammit-Mangion<sup>2</sup>, Riti Singh<sup>2</sup>, Pericles Pilidis<sup>2</sup>

**ABSTRACT:** This work describes initial results obtained from an ongoing research involving the development of optimization algorithms which are capable of performing multi-disciplinary aircraft trajectory optimization processes. A short description of both the rationale behind the initial selection of a suitable optimization technique and the status of the optimization algorithms is firstly presented. The optimization algorithms developed are subsequently utilized to analyze different case studies involving one or more flight phases present in actual aircraft flight profiles. Several optimization processes focusing on the minimization of total flight time, fuel burned and oxides of nitrogen (NO<sub>x</sub>) emissions are carried out and their results are presented and discussed. When compared with others obtained using commercially available optimizers, results of these optimization processes show satisfactory level of accuracy (average discrepancies ~2%). It is expected that these optimization algorithms can be utilized in future to efficiently compute realistic, optimal and 'greener' aircraft trajectories, thereby minimizing the environmental impact of commercial aircraft operations.

**KEYWORDS:** Trajectory optimization, Aircraft emissions, Environmental impact.

## INTRODUCTION

In this globalized world, where the efficient transportation of people and goods greatly contributes to the development of a given region or country, the aviation industry has found the ideal conditions for its development. These conditions have made the aviation industry one of the fastest growing economic sectors during the last decades. The growth in the aviation industry is reflected in the increase in air transport, expressed in terms of Revenue Passenger-Kilometers (RPKs), which has risen in an average annual rate of around 5% over the past 20 years (Boeing Commercial Airplanes, 2009). Market projections associated with this industry indicate that this growth will continue over the following years.

Environmental issues associated with aircraft operations are currently one of the most critical aspects of commercial aviation (Green, 2003; Clarke, 2003; Brooker, 2006; Riddlebaugh, 2007). These are due to both the continuing growth in air traffic and the increasing public awareness about anthropogenic contribution to global warming. The critical nature of this problem means that currently several organizations worldwide are focusing their efforts towards large collaborative projects whose main objective is to identify the best alternatives or routes to reduce the environmental impact of aircraft operations. Particular examples of these projects are Partnership for AiR Transportation Noise and Emissions Reduction (PARTNER) project (PARTNER, 2003) and European Clean Sky JTI (Joint Technology Initiative) project (Clean Sky JTI, 2008). The Clean Sky JTI project has been demonstrating and validating different technologies, thereby making a major move towards achieving

<sup>1</sup>.Pontifícia Universidade Católica do Rio de Janeiro – Rio de Janeiro/RJ – Brazil. <sup>2</sup>.Cranfield University, Cranfield – United Kingdom.

Author for correspondence: Cesar Celis | Departamento de Engenharia Mecânica | Pontifícia Universidade Católica do Rio de Janeiro – Rua Marquês de São Vicente 225, Rio de Janeiro/RJ | CEP: 22453-900 – Brazil | Email: cesar.celis@puc-rio.br

Received: 10/24/2013 | Accepted: 02/09/2014

the environmental goals set by Advisory Council for Aeronautics Research in Europe (ACARE). These targets for 2020 include reductions in carbon dioxide (CO<sub>2</sub>) and NO<sub>x</sub> emissions by 50% and 80%, respectively.

Cranfield University (CU) and other partners of the European Aviation Industry are collaboratively participating in several areas of Clean Sky JTI, including the Systems for Green Operations (SGO) Integrated Technology Demonstrator (ITD). The SGO ITD concentrates on two key areas: (1) Management of Aircraft Energy (MAE) and (2) Management of Trajectory and Mission (MTM). One of the main contributions of CU to the SGO ITD is the development of suitable computational algorithms for the management of aircraft trajectory and mission, in particular, for carrying out aircraft trajectory optimization processes. This paper focuses on the initial stages of the development of these optimization algorithms and their applications for determining theoretical optimum aircraft trajectories. The optimization algorithms developed are a part of an optimization suite known as 'Polyphemus' (oPtimisatiOn aLgorithms librarY for PHysical complEx MUlti-objective problemS).

As a part of the ongoing research about trajectory optimization, a methodology for optimizing aircraft trajectories has been initially devised. Then, Polyphemus has been developed and/or adapted for carrying out these aircraft trajectory optimization processes. Computational models simulating different disciplines, such as aircraft performance, engine performance, and formation of pollutants, have also been selected or developed as required. Simplified aircraft trajectory optimization processes have finally been carried out to evaluate the mathematical performance of Polyphemus primarily. Main results of these optimization processes are summarized in this paper.

## AIRCRAFT TRAJECTORY OPTIMIZATION

Optimization can be defined as the science of determining the best solutions for certain mathematically defined problems which are often representations of physical reality (Fletcher, 1987). There are several criteria and methodologies for classifying and solving optimization problems, respectively (Walsh, 1975; Schwefel, 1981; Bunday, 1984; Everitt, 1987; Krotov, 1996; Rao, 1996). Thus, aircraft trajectory optimization problems can be mainly classified as constrained, dynamic, optimal control, nonlinear – *the functions relating inputs (design variables) and outputs (objective functions) are unknown in this work and they are presumed to be non-linear, non-smooth, and non-differentiable* – real-valued

(mostly), deterministic (mostly), multimodal, multidimensional, and multiobjective. A number of optimization methods have been developed in the past, many of which are customized for a specific problem. Most important optimization methods can be grouped under three broad categories (Schwefel, 1981): (1) hill climbing methods (direct search methods, gradient methods and Newton methods); (2) random search methods; and (3) evolutionary methods. A detailed review of these methods can be found in Celis et al. (2009) and Celis (2010).

Evolutionary methods are inspired by nature, biological structures and processes that can be observed in natural environments for solving technical problems. They are based on Darwin's principles of species evolution reproduction cycle, natural selection and diversity by variation (Quagliarella, 1998). Most important evolutionary methods are evolutionary programming, evolution strategies, genetic programming and genetic algorithms (GAs). Among all evolutionary techniques, GAs are most widely used, and they have had a significant impact on optimization (Russell and Norvig, 2003). Like other evolutionary techniques, GAs are based on the principles of natural genetics and natural selection. Thus, basic elements of natural genetics (reproduction, crossover and mutation) are used in the genetic search procedure. Generally, evolutionary methods, in particular GAs, are robust, which help to solve problems in which the functions relating inputs to outputs are unknown and may have an unexpected behavior. In these situations, standard nonlinear programming techniques would be inefficient, computationally expensive, and in most cases, find a relative optimum that is the closest to the starting point (Rao, 1996). It has been argued (Betts, 1998) that evolutionary methods (including GAs and other techniques involving some sort of stochasticity during the optimization process) are not adequate to solve trajectory optimization problems and are computationally inferior when compared to methods that use gradient information. This inadequacy argument is originated from considering that trajectory optimization problems are not characterized by discrete variables. However, the results shown in this work highlight the fact that GAs are indeed suitable for this class of problems. Even more, for aircraft trajectory optimization involving multimodel integration, where the characteristics of the functions relating inputs to outputs are unknown, algorithms of this type appear to be the only practical alternative. A number of reasons that help support this point of view are as follows:

- GAs do not use specific knowledge of the optimization problem domain. Instead of using previously known domain-specific information to guide each step, they make random changes in their candidate solutions and then use the fitness function to determine whether those changes result in an improvement. As GAs optimization routines are both model- and problem-independent, and they allow the users to (simultaneously) run different models for simulating different disciplines, they appear to be the ideal methods.
- GAs are well-suited to solve problems where the fitness landscape is complex (discontinuous and multimodal), number of constraints and objectives are involved and the space of all potential solutions is large (particular characteristic of nonlinear problems).
- GAs make use of a parallel process of search for the optimum, which means that they can explore the solution space in multiple directions at once. If one path turns out to be a dead end, they can easily eliminate it and progress in more promising directions, thereby increasing the chance of finding the optimal solution.

From four main evolutionary algorithms, GAs have been initially chosen because of their large number of previous successful applications, worldwide. However, it is important to highlight that the hybridization of GAs with other optimization techniques has also been considered. This is due to fact that although GAs are an extremely efficient optimization technique, they are not the most efficient for the entire search phases (Rogeró, 2002). Thus, hybrid optimization methods will be developed in future, as they have the potential to improve the performance in a given search phase; for example, GAs techniques involving the use of both a random search phase during the beginning of the optimization process (to increase the quality of the initial population) and a hill climbing phase at the end of the optimization (to refine the quality of the optimum point once the global optimum region has been found).

### STATUS OF OPTIMIZATION ALGORITHMS (POLYPHEMUS)

Different numerical methods that could be used for solving the aircraft trajectory optimization problem were firstly reviewed, and a suitable optimization technique was initially selected (see "Aircraft Trajectory Optimization" section). The next step in the development of Polyphemus was reviewing the track record

of optimizers developed by CU for a range of applications, and identifying a candidate which could be used as a suitable 'starting point'. This resulted in the decision to use GA-based optimization routines developed by Rogeró (2002) as the basis for the development of Polyphemus. Rogeró's optimizer already includes several algorithms for each of the main phases involved in a GA-based optimization process; however, there are additional enhancements that can be introduced to further improve the quality of the optimizer. These improvements include the use of adaptive GAs (e.g., 'master-slave' configurations), which would allow using optimum GA parameters (e.g., population size, crossover ratio, mutation ratio, etc.) during the optimization processes; and also inclusion of the concept of Pareto optimality (Pareto fronts), which would improve its capabilities when performing multiobjective optimization processes. These improvements can be made based on successful past experiences of these concepts as part of previous optimizers (Gulati, 2001; Sampath, 2003) developed by CU.

As the development of Polyphemus is continuous, only a brief description of the main aspects characterizing its current status is presented here. Polyphemus has been implemented using Java as the main programming language. Its core has been developed based on the basic structure of 'SGA Java V1.03' from Hartley (1998), which involves a Java implementation of the 'simple GA' (SGA) from Goldberg (1989). However, the original model has been recoded and extensively modified to both adapt to engineering design optimization problems and to maximize its performance. The main modifications made help to improve both the optimization performance, through an adaptation to the application domain, and the technique and genetic operators utilized during the optimization process. The optimizer application domain considered was engineering design. Thus, the chromosome modules have been developed in a way to support real-number parameter encoding in conjunction with a defined allowable range for the parameters (genes). In addition, algorithms for keeping a historical record of all created chromosomes and for preventing the creation of duplicate ones have been implemented. In order to improve the GA technique, concepts such as elitism (preservation of the genetic material of the best members through generations), steady-state replacement (partial replacement of the newly-generated chromosomes to avoid loss of potentially good genetic material), and fitness scaling (trade-off between premature convergence and genetic drift by keeping the selection pressure relatively constant along the whole optimization process) have been introduced.

Another phase of the optimization performance improvement involved the implementation of more advanced and efficient GA operators (crossover, mutation and selection) (Rogero, 2002). Thus, several crossover techniques suitable for real-number encoding have been implemented, including weighted averaging crossover method, blend crossover BLX-a method and simulated binary crossover SBX method. The simulated binary crossover SBX method involves the creation of solutions within the whole search space. For instance, for a problem with ' $k$ ' design variables (or genes), a real-number vector (chromosome) can be given by:

$$X = \{x_1, x_2, x_3, \dots, x_k\} \quad (1)$$

Then, one of the most simple ways of performing a crossover operation using any two parent chromosomes,  $X_1$  and  $X_2$ , involves the combination of the two vectors representing them, which is as follows:

$$\begin{aligned} X'_1 &= \lambda_1 X_1 + \lambda_2 X_2 \\ X'_2 &= \lambda_1 X_2 + \lambda_2 X_1 \end{aligned} \quad (2)$$

Here, the multipliers  $\lambda_1$  and  $\lambda_2$  (subject to the condition  $\lambda_1 + \lambda_2 = 1$ ) represent the weights randomly selected during the crossover process, and  $X'_1$  and  $X'_2$  are the child chromosomes. Depending on the permissible values of the multipliers  $\lambda_1$  and  $\lambda_2$ , different subtypes of crossover methods can be derived. The (weighted) averaging crossover corresponds to the special case, in which  $\lambda_1 = \lambda_2 = 0.5$ . The averaging crossover suffers from contraction effects because it allows the creation of offspring only along the line generated between the two parental chromosomes. This problem is solved to some extent in the blend crossover BLX-a method, which uses an exploration factor ( $\alpha$ ) to increase the exploration capability of the crossover operator.

In addition to the standard random mutation operator, others such as creep mutation, with and without decay, and Dynamic Vektored Mutation (DVM) – have also been implemented. In general, for a given parent chromosome  $X$ , Eq. (1), if its element (gene)  $x_i$  is selected for mutation, a (random) change in the value of this selected gene within its domain, given by a lower  $LB_i$  and upper  $UB_i$  bound, will result in the following transformation:

$$\begin{aligned} \{x_1, x_2, x_3, \dots, x_i, \dots, x_k\} &\rightarrow \{x_1, x_2, x_3, \dots, x'_i, \dots, x_k\} \\ x_i, x'_i &\in [LB_i, UB_i] \end{aligned} \quad (3)$$

As creep mutation is basically operated by adding or subtracting a random number to a gene of the chromosome selected for mutation, the mutation of a given gene,  $x_i$ , using this method is limited to a creep range centered on its original value (Davis, 1991). A creep mutated gene,  $x'_i$ , is then computed as follows:

$$x'_i = x_i + (2r - 1)\Delta_{\max}, \text{ where} \quad (4)$$

$$\Delta_{\max} = \delta.(UB_i - LB_i) \quad (5)$$

In Eqs. (4) and (5),  $\Delta_{\max}$  is the maximum size used for the creep mutation,  $\delta$  is the range ratio, and  $r$  is a random number from  $[0,1]$ . The level of disruption produced by the mutation process is controlled by the creep size  $\delta$ . In the creep mutation with decay method, the creep size is altered as a function of the stage of the search process as follows:

$$\delta_{t+1} = \delta_t(1 - \gamma) \quad (6)$$

In Eq. (6),  $\gamma$  represents the creep decay rate and  $t$  is the generation number. This type of implementation allows the use of large values of  $\delta$  in the beginning of the search process and small values at the end; the exploration and exploitation capabilities required during the process are balanced in this way. Details about the DVM method can be found in Rogero (2002).

Selection operators implemented in the optimizer include a modified roulette wheel selection operator (limiting the number of chromosome instances) and the Stochastic Universal Sampling (SUS) technique. Roulette wheel selection, in which an area proportional to its fitness is allocated to each chromosome on a virtual roulette wheel, is the best known selection method. The selection process is carried out by spinning the wheel a number of times equal to the number of chromosomes to be selected (each time a single chromosome is selected). One drawback associated with this selection method is that it has a tendency to select a large number of copies of the best chromosome, which can lead to loss of diversity. This problem can be solved to some extent by using the SUS selection method. In this method, like in the roulette wheel selection, a chromosome occupies on the wheel an area proportional to its fitness. However, instead of spinning the wheel several times for selecting chromosomes, a single spin of the wheel identifies all parent selections simultaneously. This is possible because there is another wheel on the outside of the

roulette wheel containing a number of equally spaced pointers equal to the number of chromosomes to be selected (Callan, 2003). With regard to replacement operators, tournament replacement and ranked replacement have been improved and implemented as replacement operators.

Finally, Polyphemus uses a unique optimization method based on Wienke's idea of target vector optimization (Wienke *et al.*, 1992). In this method, designers can define, for each parameter, a target to be attained, a range within which this parameter should remain, and the requirement to maximize or minimize the given parameter. Accordingly, the quality of the design is determined by the level of both the achievement of the targets and the violation of the parameters ranges. This approach enables designers to have total control over the optimization process with neither having to know much about the optimization algorithms, nor having to devise a fitness function (Rogerero and Rubini, 2003). The optimization results presented in the following sections were obtained using the current version of Polyphemus, whose main characteristics have been summarized above.

## TRAJECTORY OPTIMIZATION CASE STUDIES

In this section, computational models utilized, flight profiles optimized and the methodology followed for optimizing these flight profiles have been particularly emphasized.

## Computational Models

In the aircraft trajectory optimization processes, three computational models, i.e., aircraft performance simulation model (APM), engine performance simulation model (TurboMatch) and emissions prediction model (Hephaestus), have been utilized. Figure 1 illustrates the general arrangement of these models, as well as different parameters exchanged among them. The APM (Long, 2009) is a generic tool that determines flight path performance for a given aircraft design. It uses steady-state performance equations to resolve aerodynamic lift and drag and to determine the thrust required for a given kinematic flight state. In order to easily identify the behavior of Polyphemus, airspeed limitations – such as critical Mach number ( $M$ ), never-exceed speed and wave drag at transonic  $M$  – have not been implemented in the model. As APM uses endpoints to compute performance, the user must declare a trajectory segment in terms of ground range and altitude intervals, whereby a constant flight path angle is then defined. Flight conditions are then assumed to be constant over that segment. The aircraft modeled in this work corresponds to a typical mid-sized, single-aisle, twin turbofan airliner with a maximum takeoff weight (MTOW) of about 72,000 kg and a seating capacity of about 150 passengers.

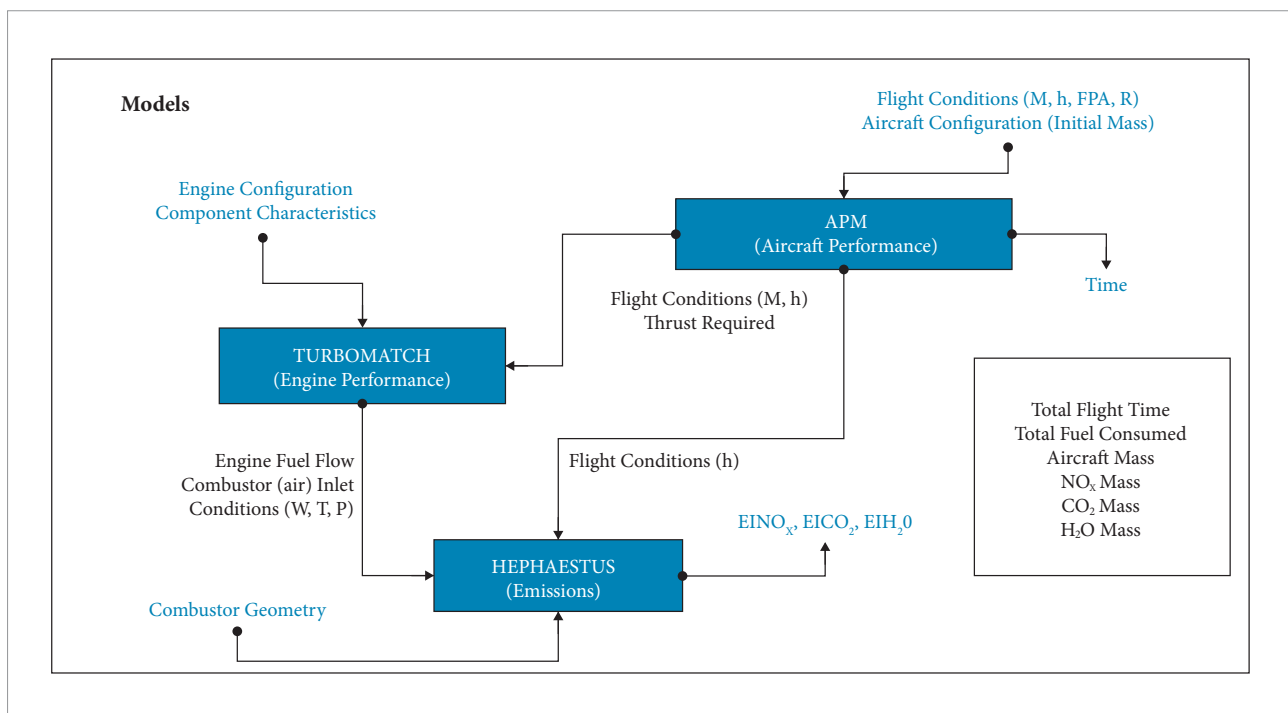


**Figure 1.** Computational models configuration and exchange of parameters.



The performance of the engines was simulated using TurboMatch (Palmer, 1999), which is the in-house CU gas turbine performance code that has been developed and refined over a number of decades. TurboMatch performance simulations range from simple steady-state (design and off-design point) to complex transient performance computations. Finally, the gaseous emission predictions have been performed using the CU emissions prediction software, Hephaestus. An integral part of Hephaestus constitutes the emissions prediction model described in Celis *et al.* (2009), which follows an approach based on the use of a number of stirred reactors for modeling combustion chambers and estimating the level of pollutants emitted from them. Additional details of these computational models can be found in Celis *et al.* (2009) and Celis (2010).

### Flight Profiles

It is clear that in order to demonstrate the suitability of an optimizer for optimizing aircraft trajectories, an extensive validation process of the algorithms that are implemented needs to be carried out using different analytical problems with known optimal values. In the case of Polyphemus, this part of the validation process has already been performed (Rogerio, 2002) and is therefore not repeated here. In order to provide insight into the results that can be expected using Polyphemus, simplified aircraft trajectory optimization processes using this optimizer have been performed. It is relevant to note that the main objective of these processes was evaluation of the mathematical performance of Polyphemus rather than the generation of realistic aircraft trajectories. Consequently, simplifications (in terms of number of flight segments, design variables, constraints and objective functions, etc.) have been introduced when optimizing the aircraft flight profiles. Indeed, the results discussed in this work correspond to single-objective optimization processes only, which means that the determination of non-dominated or Pareto optimal solutions that characterize multi-objective optimization processes is out of the scope of this work.

In this work, the aircraft flight profiles have been divided into only a small number of segments, as illustrated in Fig. 2. This helps getting a greater visibility on the characteristics of the Polyphemus performance when assessing results. This would have been more difficult if the trajectory had been divided into a greater number of segments. These hypotheses are a simplification of real cases but provide numerical solutions that are used to commission the methodology. In order to obtain meaningful results in terms of actual optimum trajectories, the flight path needs to be divided into a much larger number of segments, each small enough so

that the errors associated with the assumptions made within each segment will be cumulatively insignificant. All the optimization processes carried out involved only vertical profiles. Therefore, only three parameters have been used to define a given aircraft trajectory: (1) flight altitude ( $h$ ); (2) aircraft speed: true airspeed (TAS), equivalent airspeed (EAS) or Mach number ( $M$ ); and (3) range ( $R$ ): the horizontal distance flown by the aircraft. One of the main uses of Polyphemus involves the optimization of aircraft trajectories between city pairs. Thus,  $R$  has been usually kept constant during the optimizations, and only altitude and aircraft speed vary (i.e., used as design variables) to compute optimum aircraft trajectories that minimize, separately, total flight time, fuel burned and  $\text{NO}_x$  emissions.

Several aircraft flight profiles have been optimized in order to assess the mathematical performance of Polyphemus. The optimization results associated with three of these flight profiles are summarized in this paper. A brief description of these profiles, which were analyzed as part of three separate case studies, is presented as follows:

- *Case 1: Simple Climb Profile Optimization.* (i) Flight profile has been divided into four segments (Fig. 2). (ii) Climb segments have been defined by arbitrary segment lengths (range,  $R$ ). (iii) Overall climb has been defined by the cumulative range, start and end altitudes, and Mach numbers. (iv) Variation in intermediate Mach numbers (initial  $M$  in segments 2 and 3) and altitudes (initial altitude in segments 2, 3 and 4) has been allowed during the optimization processes. (v) Only explicit constraints have been utilized, i.e., range of permissible values of the design variables ( $h$  and  $M$ ) are limited. (vi) Lower and upper bounds for these permissible ranges have been set at 457 m (1,500 ft) and 10,668 m (35,000 ft), respectively, for  $h$  (profile start and end altitudes); and 0.38 and 0.80, respectively, for  $M$ . (vii) International Standard Atmosphere

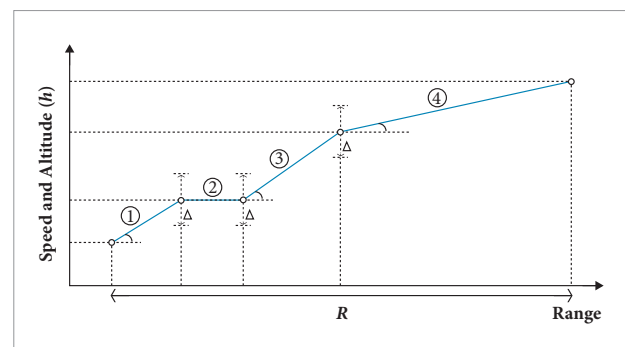


Figure 2. Generic aircraft flight profile.

(ISA) conditions are assumed. (viii) Range of flight path angle (FPA) allowed:  $[0, 7.5]$  deg. Data corresponding to this particular profile optimization are summarized in Table 1.

- *Case 2: Implicitly Constrained Climb Profile Optimization.* (i) Flight profile is similar to the profile used in Case 1; however, aircraft speeds have been specified at the start and end of each climb segment allowing continuity in aircraft speed. (ii) Climb schedule has been described as follows; 1st seg.: climb at constant EAS from 1,500 ft (457 m) up to 10,000 ft (3,048 m); 2nd seg.: EAS acceleration at 10,000 ft (level flight); 3rd seg.: climb at constant EAS up to a segment final altitude where (cruise)  $M$  is about 0.8; 4th seg.: climb at constant  $M$  from this altitude up to 35,000 ft (10,668 m). (iii) Design variables and their range of permissible values: initial EAS in segment 1 ( $EAS_{i1}$  [89.0, 128.6] m/s), final EAS in segment 2 ( $EAS_{2f}$  [133.8, 221.2] m/s), initial altitude in segment 3 ( $h_{3i}$  [3048, 4400] m), and initial altitude in segment 4 ( $h_{4i}$  [3048, 10668] m). (iv) Implicit constraint: initial  $M$  in segment 4 ( $M_{4i}$ ) – allowable range  $\pm 0.5\%$  of its nominal value, 0.8. (v) ISA conditions have been assumed. (vi) FPA range allowed:  $[0, 7.5]$  deg. Additional details about this case study are shown in Table 2.
- *Case 3: Quasi-Full Flight Profile Optimization.* (i) Flight profile (involving climb, cruise and descent) has been divided into eight segments. (ii) Profile has been defined following a similar approach to that used in Case 2. (iii) Flight schedule has been described as follows; 1st seg.: climb at constant EAS

from 1,500 ft (457 m) up to 10,000 ft (3,048 m); 2nd seg.: EAS acceleration at 10,000 ft (level flight); 3rd seg.: climb at constant EAS up to a segment final altitude where (cruise)  $M$  is about 0.8; 4th and 5th seg.: level flight cruise at constant  $M$ ; 6th seg.: descent at constant EAS to 10,000 ft (3,048 m); 7th seg.: EAS deceleration at 10,000 ft (level flight); and 8th seg.: descent at constant EAS from 10,000 ft (3,048 m) to 1,500 ft (457 m). (iv) Design variables and their range of permissible values: initial EAS in segment 1 ( $EAS_{i1}$  [89.0, 128.6] m/s), final EAS in segment 2 ( $EAS_{2f}$  [117.1, 184.6] m/s), initial altitude in segment 3 ( $h_{3i}$  [3048, 4400] m), initial altitude in segment 4 ( $h_{4i}$  [6096, 12192] m), initial altitude in segment 7 ( $h_{7i}$  [3048, 4400] m), and initial EAS in segment 8 ( $EAS_{8i}$  [89.0, 128.6] m/s). (v) Implicit constraint: initial  $M$  in segment 4 ( $M_{4i}$ ) – allowable range  $\pm 0.5\%$  of its nominal value, 0.8. (vi) ISA conditions have been assumed. (vii) FPA range allowed:  $[0, 7.5]$  deg during climb and cruise, and  $[-7.5, 0]$  deg during descent. Table 3 summarizes the data associated with this flight profile optimization.

The lower and upper bounds of the range of permissible values of the design variables were in general defined in a way to reduce the computational time of the optimization processes, to take into account typical air traffic control (ATC) restrictions, and/or to avoid the aircraft losing (gaining) altitude during climb (descent) processes. For instance, below 10,000 ft, the EAS lower and upper bounds usually correspond to, respectively, the aircraft stall speed (89.0 m/s

**Table 1.** Case 1 (simple climb profile) – Baseline trajectory and design variables.

| Seg. No. | $h_i$ (m) | $h_f$ (m) | $M$  | $R$ (km) | Design variables                                      |
|----------|-----------|-----------|------|----------|---|
| 1        | 457       | 3048      | 0.38 | 20       | –   |
| 2        | 3048      | 3048      | 0.46 | 10       | $0.38 \leq M_i \leq 0.80$ ; $457 \leq h_i \leq 10668$ |
| 3        | 3048      | 7000      | 0.58 | 60       | $0.38 \leq M_i \leq 0.80$ ; $457 \leq h_i \leq 10668$ |
| 4        | 7000      | 10668     | 0.80 | 100      | $457 \leq h_i \leq 10668$                             |

**Table 2.** Case 2 (implicitly constrained climb profile) – Baseline trajectory and design variables.

| Seg. No. | $h_i$ (m) | $h_f$ (m) | $M_i$ | $M_f$ | $EAS_i$ (m/s) | $EAS_f$ (m/s) | $R$ (km) | Design variables              |
|----------|-----------|-----------|-------|-------|---------------|---------------|----------|-------------------------------|
| 1        | 457       | 3048      | –     | –     | 128.6         | 128.6         | 20       | $89.0 \leq EAS_i \leq 128.6$  |
| 2        | 3048      | 3048      | –     | –     | 128.6         | 164.6         | 10       | $133.8 \leq EAS_f \leq 221.2$ |
| 3        | 3048      | 7724      | –     | –     | 164.6         | 164.6         | 60       | $3048 \leq h_i \leq 4400$     |
| 4        | 7724      | 10668     | 0.80  | 0.80  | –             | –             | 100      | $3048 \leq h_i \leq 10668$    |

**Table 3.** Case 3 (quasi-full flight profile) – Baseline trajectory and design variables.

| Seg. No. | $h_i$ (m) | $h_f$ (m) | $M_i$ | $M_f$ | $EAS_i$ (m/s) | $EAS_f$ (m/s) | R (km) | Design variables              |
|----------|-----------|-----------|-------|-------|---------------|---------------|--------|-------------------------------|
| 1        | 457       | 3048      | –     | –     | 128.6         | 128.6         | 20     | $89.0 \leq EAS_i \leq 128.6$  |
| 2        | 3048      | 3048      | –     | –     | 128.6         | 164.6         | 10     | $117.1 \leq EAS_i \leq 184.6$ |
| 3        | 3048      | 7724      | –     | –     | 164.6         | 164.6         | 160    | $3048 \leq h_i \leq 4400$     |
| 4        | 7724      | 7724      | 0.80  | 0.80  | –             | –             | 230    | $6096 \leq h_i \leq 12192$    |
| 5        | 7724      | 7724      | 0.80  | 0.80  | –             | –             | 230    | –                             |
| 6        | 7724      | 3048      | –     | –     | 164.6         | 164.6         | 140    | –                             |
| 7        | 3048      | 3048      | –     | –     | 164.6         | 128.6         | 20     | $3048 \leq h_i \leq 4400$     |
| 8        | 3048      | 457       | –     | –     | 128.6         | 128.6         | 70     | $89.0 \leq EAS_i \leq 128.6$  |

$EAS$  for the particular aircraft modeled) and the maximum  $EAS$  permissible below this altitude (according to ATC restrictions), i.e., 250 kts  $EAS$  or 128.6 m/s. In Case 3, in particular, the range of values in which the initial altitude in segment 4 can vary was established in a way to allow the aircraft cruising at altitudes between 20,000 ft (6,096 m) and 40,000 ft (12,192 m). Thus,  $EAS_{2f}$  permissible values were limited to those speeds that yield Mach numbers of about 0.8 at these cruise altitudes. Similar considerations were made in the other case studies analyzed in this work.

### Optimization Process

According to the methodology followed in this work for optimizing a given aircraft trajectory, Polyphemus first randomly changes the values of the design variables (altitude and/or aircraft speed in one or more trajectory segments) in order to create a group of potential solutions. For a given potential solution, by making use of the initial aircraft weight (aircraft empty weight plus fuel on-board, constant), the APM carries out the computations related to the first segment of the aircraft trajectory, and determines the thrust required, flight time, etc. (Fig. 1). TurboMatch subsequently uses the flight conditions and the thrust required to determine the engine operating point, thereby establishing the engine fuel flow and the combustor inlet conditions among others. Hephaestus then makes use of the combustor inlet conditions and combustor geometric parameters to calculate the emission indices for the main pollutants. Based on the fuel flow and flight time, the fuel burned during the first trajectory segment and the new aircraft weight (i.e. the initial weight less fuel burned) are calculated. Computations continue in a similar fashion for all the remaining trajectory segments. When all the segments have been computed, among other calculations, the total flight time, fuel burned and gaseous

emissions produced during the whole aircraft trajectory are also computed. This process is repeated for all the potential solutions, and for all generations of potential solutions that Polyphemus utilizes in order to determine an optimum trajectory according to given criteria initially specified by the designer. The results were obtained following a procedure similar to that described before.

## RESULTS AND DISCUSSIONS

Main results of the optimization processes corresponding to three case studies indicated above are summarized in this section. In these processes, the minimization of total flight time, fuel burned, and  $NO_x$  emissions have been considered as the objective functions.

### Case 1: Simple Climb Profile Optimization

The baseline climb profile for this case study as well as the optimum trajectories computed using Polyphemus and two commercial optimizers (MATLAB®, 2008) are illustrated in Fig. 3. Two different approaches used within the commercial package were (i) a pattern search algorithm called mesh adaptive search (MADS), and (ii) GAS. Both Polyphemus and the commercial optimizers yielded very similar results (Fig. 3a). Even though this first optimization case study (climb profile) corresponded to a hypothetical one, the reasonable agreement among the optimizers (average discrepancies ~2%) confirmed the validity of the approach. Figure 3c shows that in order to minimize the time spent during climb, Polyphemus suggests a solution where the aircraft flies at the highest  $M$  permissible, which was fixed at 0.38 and 0.80 in the first and fourth segment, respectively, and free to rise to 0.8 in the remaining middle two. Polyphemus also



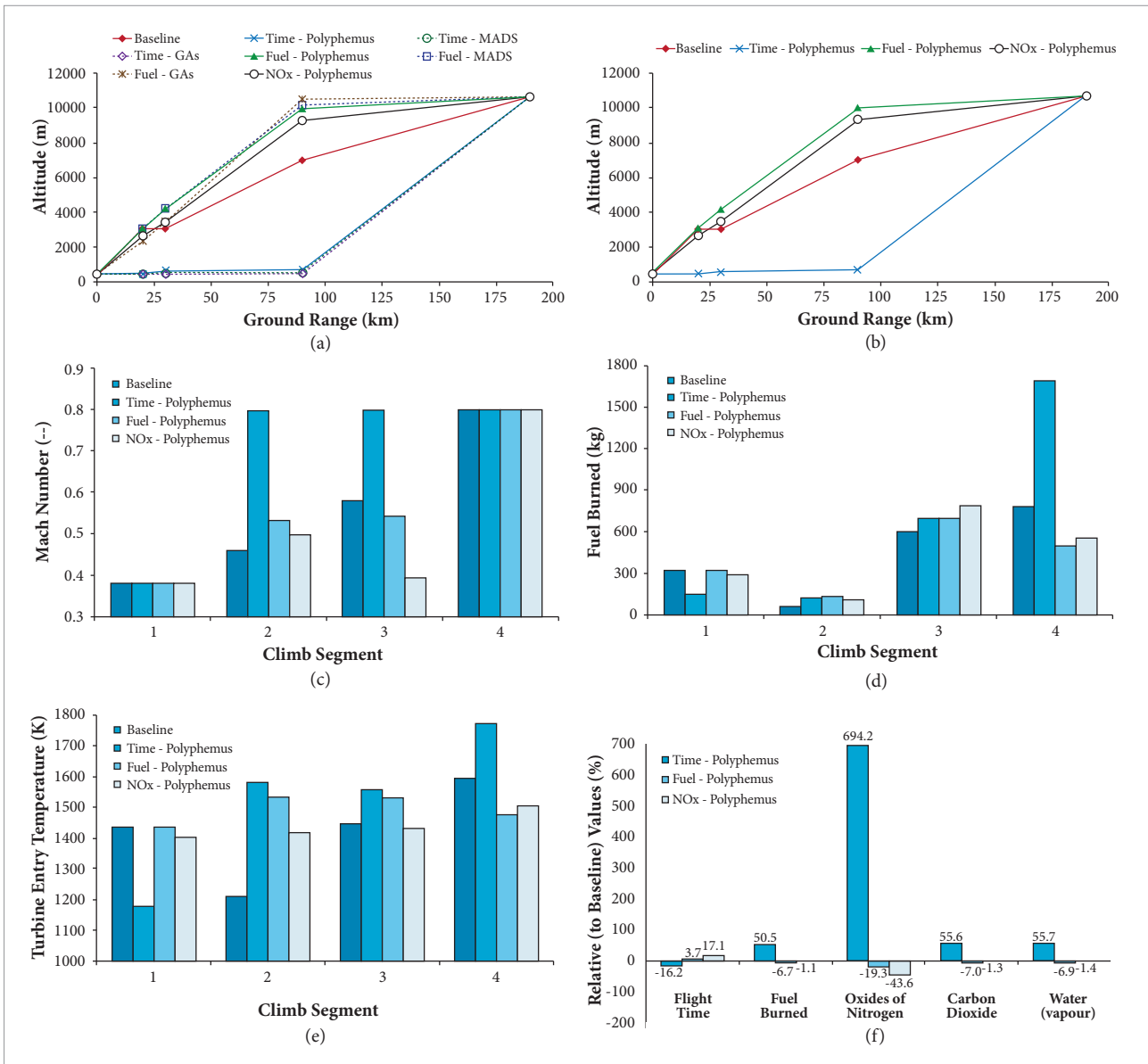


Figure 3. Case 1 – Simple climb profile optimization results.

suggests that the aircraft should fly at low altitudes for as long as possible before climbing rapidly to the target end altitude (Fig. 3b). This is mathematically correct because the speed of sound is the highest at sea level, thus enabling the aircraft to fly faster (maximization of TAS) if it could actually achieve  $M$  0.8 at this level. This solution, however, does not represent practical flight profiles because never exceed speed ( $V_{NE}$ ) is much lower than  $M$  0.8 at sea level, thus restricting large transport category aircraft from approaching such high Mach numbers. Nevertheless, it is an interesting solution, confirming that the optimizer is working correctly in the absence of  $M$  (or TAS) constraints.

Figure 3 also illustrates that in order to reduce fuel burn, the optimizer suggests flying slower (Fig. 3c) and higher (Fig. 3b) than the reference trajectory (segment 3). This is again conceptually correct given the current reference trajectory. It is interesting to note that the fuel-optimized trajectory proposes second and third segments affording a greater fuel burn (relative to the baseline) (Fig. 3d) in order to gain height (Fig. 3b), which then subsequently yields a lower fuel burn in the last segment and an overall lower fuel burn for the climb profile as a whole. In terms of flight profile, one could conclude from Fig. 3b that the trajectories optimized for minimum fuel burned and  $NO_x$  emissions are similar. However,

there are significant differences between these two trajectories. The main difference is related to the fact that the  $\text{NO}_x$  emissions optimized trajectory is flown at relatively lower Mach numbers than the fuel burned optimized trajectory (Fig. 3c). These lower Mach numbers result in lower engine thrust settings, i.e., the thrust required to fly a given segment is lower, which in turn results in lower engine turbine entry temperature (TET) values (Fig. 3e). Consequently, as one of the main factors determining the level of  $\text{NO}_x$  emissions produced (besides the fuel burned) is TET, the trajectory optimized for minimum  $\text{NO}_x$  emissions produces a significant reduction in the amount of  $\text{NO}_x$  emitted (~43%). Interestingly, Fig. 3e shows that in order to minimize  $\text{NO}_x$  emissions, the optimizer proposes a trajectory in which the engine TET remains almost constant (~1,400–1,500 K) for the entire climb profile. It is relevant to note in this discussion that the level of  $\text{NO}_x$  formed at temperatures near to and above 1,700–1,800 K increases exponentially with temperature.

An aspect to be highlighted in Fig. 3f is the level of gaseous emissions ( $\text{NO}_x$ ,  $\text{CO}_2$  and  $\text{H}_2\text{O}$ ) associated with the optimum trajectories relative to the reference climb trajectory. As expected, variations in  $\text{CO}_2$  and  $\text{H}_2\text{O}$  are directly proportional to the variations in the amount of fuel burned (species in chemical equilibrium). However, the aircraft trajectory optimized for total flight time significantly increases the amount of  $\text{NO}_x$  emissions. One of the main factors responsible for this significant increase in  $\text{NO}_x$  emissions (besides the increase in fuel burn) is the increase in TET resulting from the higher thrust settings. Fig. 3f also illustrates the increase in total flight time associated with the trajectory optimized for minimum  $\text{NO}_x$  emissions. Although this parameter increases, the total fuel burned slightly decreases as a consequence of the lower thrust settings (i.e., lower engine fuel flow relative to the baseline trajectory). Additional details about the results analyzed in this first case study can be found in Celis *et al.* (2009). In the following two case studies, complexities (in terms of operational constraints, number of segments, number of trajectory flight phases, etc.) were included gradually. This gradual approach afforded greater visibility of the mathematical performance of Polyphemus when assessing results, which would have been more difficult if the analysis had been initiated with very complex trajectories.

### Case 2: Implicitly Constrained Climb Profile Optimization

Results obtained in the second case study (Fig. 4) are in general similar to those obtained in the first case study. Thus, when minimizing the time spent during climb, i.e., maximizing

TAS, Polyphemus suggests a solution where the aircraft flies the first segment at the highest EAS permissible (fixed at 128.6 m/s) (Fig. 4c). This is conceptually correct because in the first segment, since the flight altitude is fixed, TAS increases with the increase in EAS. The optimizer also suggests that the aircraft should accelerate in the second segment to the highest EAS permissible (fixed at 221.2 m/s), and fly the following segments at low levels (Fig. 4b) as long as possible before climbing rapidly to the target end altitude. This is again mathematically correct because, firstly, as previously indicated, once the flight altitude has been established, the TAS increases with increase in EAS; and, secondly, for a given  $M$ , TAS increases with the decrease in altitude (speed of sound is the highest at sea level). Clearly, the influence of the third and fourth segments on the total climb time is more important than the corresponding second segment. Otherwise, the initial altitude in segment 3 would be the highest permissible.

Figure 4 also shows that in order to reduce the climb fuel burned, Polyphemus suggests flying mostly slower (Fig. 4c) and higher (Fig. 4b) than the reference trajectory. In particular, it suggests flying the first segment at the highest EAS permissible. It is clear that in order to minimize the total amount of fuel burned, the total energy required by an aircraft to describe a given flight profile (aircraft energy change plus path-dependent energy required to impart that change) must be minimized. Thus, in this particular case, the total energy required to climb must also be minimized. It means that the total aircraft kinematic energy change needs to be minimized. The aircraft kinetic energy change is minimized when the initial kinetic energy is maximized. It implies, in turn, maximization of the initial aircraft speed, i.e., TAS. This TAS maximization results in the maximization of the EAS at the first segment, as highlighted. One of the main factors driving the minimization of the fuel burned during a given flight profile is the aircraft mass change. Different factors affect the fuel burned and, consequently, the changes in the aircraft mass. The aircraft speed and flight altitude constitute two of these main factors. Reducing the speed and increasing the altitude reduce drag and, consequently, the thrust required to fly a given segment. This lower thrust requirement translates into a lower engine thrust setting, and, consequently, a lower fuel burn. However, neither altitude nor speed can be increased or decreased arbitrarily. Speed reductions imply in general, an increase in flight time, which can negatively affect the total fuel burned. In addition, in order to quickly achieve higher altitudes, higher engine thrusts (i.e. higher thrust settings) are required. These higher thrust settings require higher fuel flow, which

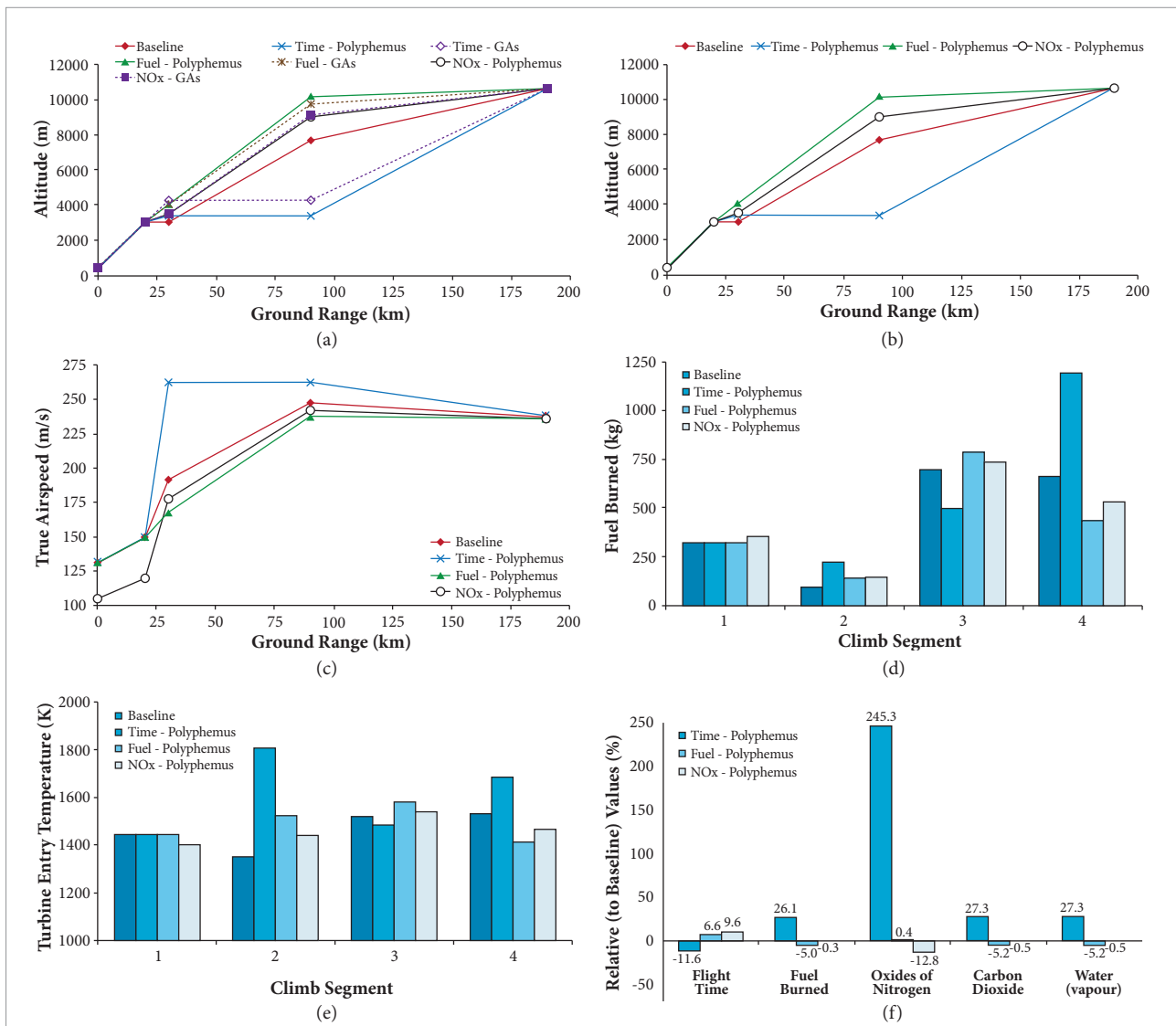


Figure 4. Case 2 – Implicitly constrained climb profile optimisation results.

negatively affects the fuel burned during the process. Therefore, a compromise between aircraft flight altitude and speed, which directly affect the changes in the aircraft mass, needs to be achieved at some stage. The fuel-optimized trajectory computed is a typical example of the referred compromise. It is interesting to note in Fig. 4d that this fuel-optimized trajectory proposes second and third segments affording a greater fuel burn (relative to the baseline) in order to gain height (Fig. 4b), which, then, is translated into a lower fuel burn in the last segment and an overall lower fuel burn for the whole climb profile.

Regarding the trajectory optimized for minimum  $\text{NO}_x$  emissions, the results show that, similar to the fuel optimized one, this trajectory

is flown mostly slower (Fig. 4c) and higher (Fig. 4b) than the baseline trajectory. In general, lower speed and higher altitude lead to a reduction in the thrust required to fly the climb segments. These lower thrust requirements are in turn translated into lower engine TET values (Fig. 4e), which in turn result in a reduction in the level of  $\text{NO}_x$  emissions (Fig. 4f). As in the first case study, Fig. 4e illustrates that in order to minimize  $\text{NO}_x$  emissions, the aircraft describes a trajectory in such a way that the engine TET remains almost constant along the whole climb profile. As before,  $\text{CO}_2$  and  $\text{H}_2\text{O}$  vary proportionally to the variations of fuel burned (Fig. 4f). Even though the  $\text{NO}_x$  emission-optimized trajectory increases total flight time, as a consequence of the lower engine thrust settings

utilized, the total amount of fuel burned is slightly reduced. In Fig. 4f, it should also be noticed that the aircraft trajectory optimized for minimum flight time significantly increases the amount of NO<sub>x</sub> emissions. This is partially because of the large amount of thrust required to increase both aircraft kinetic energy in segment 2 and potential energy in segment 4. This higher engine thrust requirement is translated into higher TET values (Fig. 4e), and consequently into a significant increase in the level of NO<sub>x</sub> emissions.

*Case 3: Quasi-Full Flight Profile Optimization*

As highlighted before and illustrated in Fig. 5, which shows the main results obtained for this particular case study, minimization of total flight time implies maximization of TAS (Fig. 5c).

Thus, when determining the minimum flight time-optimized trajectory, Polyphemus suggests a solution in this case, where the aircraft flies the first and the last segments at the highest EAS permissible (fixed at 128.6 m/s). This is conceptually correct because the first and last segments are flown at fixed altitudes, where TAS increases with the increase in EAS. Polyphemus also suggests that the aircraft should accelerate in the second segment to the highest EAS permissible (fixed at 184.6 m/s), and start the third segment as high as possible, and the fourth one as low as possible. This is again mathematically correct because, firstly, TAS increases with the increase in both flight altitude and EAS (segments 2 and 3); and, secondly, for a given Mach number, the TAS increases with the decrease in altitude (segments 4 and 5).

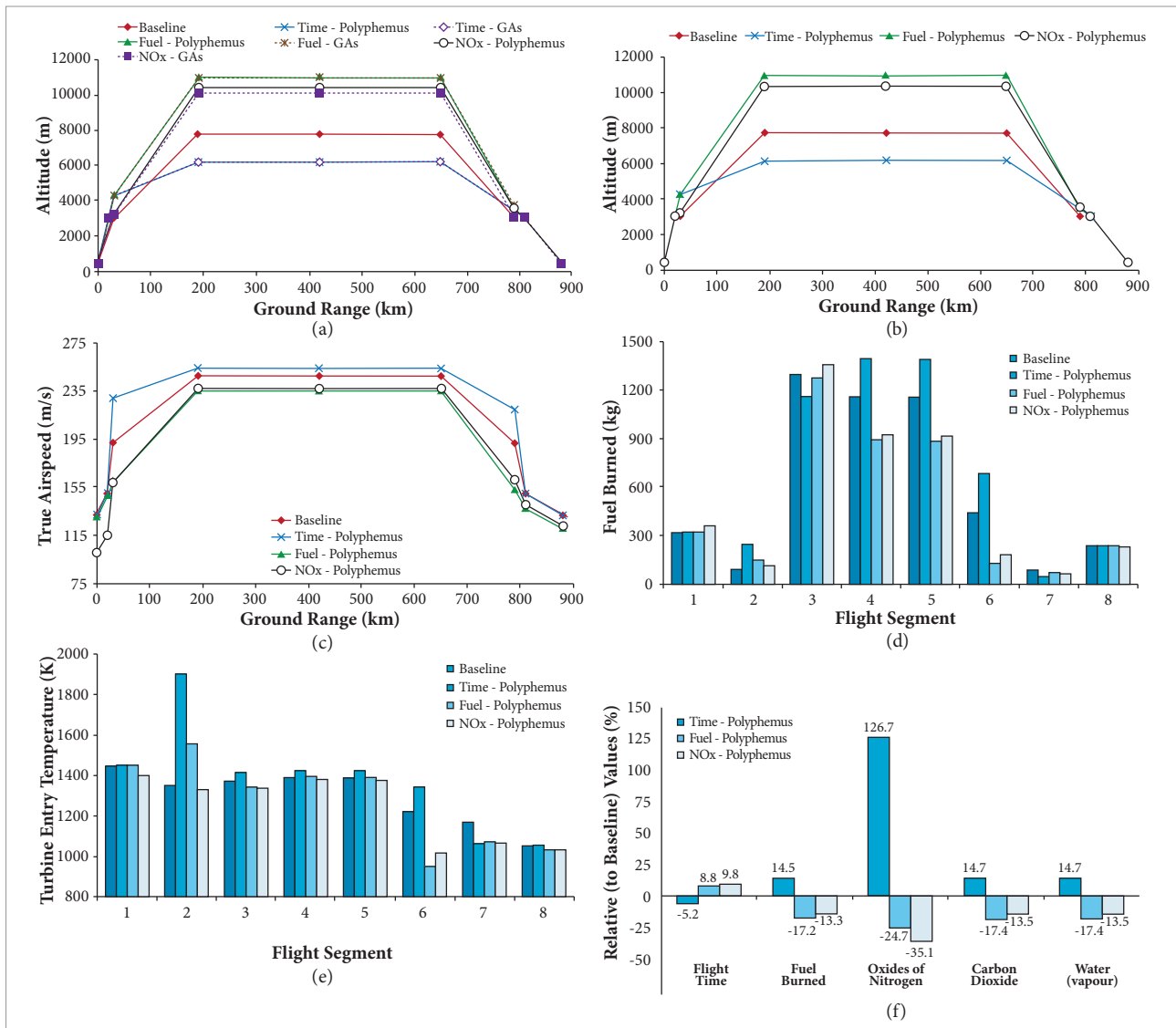


**Figure 5.** Case 3 – Quasi-full flight profile optimization results.

As a consequence of the larger distance covered by the cruise segments 4 and 5, their influence on the total flight time is more important than that associated with the third and sixth segments. This is emphasized by the fact that the aircraft has a tendency to cruise at low altitude levels as observed in Fig. 5b.

Regarding the fuel-optimized trajectory, it is observed that in order to reduce the total fuel burned, the optimiser suggests flying mostly slower (Fig. 5c) and higher (Fig. 5b) than the reference trajectory. In particular, it suggests flying the first segment at the highest EAS permissible. This situation is similar to that encountered in the second case study. In order to minimize the total fuel burned during the flight profile, the total energy required during the process must be minimized. In this case, it implies, in turn, minimization of the aircraft kinetic energy change; or, more specifically, maximization of the initial aircraft speed and minimization of the final one (in terms of TAS). As in the second case study, this TAS maximization makes the aircraft fly the first segment at the highest EAS permissible. Results also show that even though the aircraft arrives to the endpoint at a low speed, this does not correspond to the lowest EAS permissible (fixed at 89.0 m/s), as it could be expected. It is believed that one aspect that might be influencing this particular result is the path-dependent energy, which has a direct relationship with the aircraft speed and also needs to be minimum. In the foregoing analysis, the aircraft mass changes were not considered. These mass changes cannot be ignored however because in reality they are one of the main factors driving the minimization of the fuel burned during the optimization process. As highlighted before, there are two main parameters that affect the fuel burned and, consequently, the changes in the aircraft mass: the aircraft speed and the aircraft flight altitude. These two parameters directly or indirectly affect, in turn, other parameters, such as drag, thrust required, flight time and engine thrust setting (consequently, fuel flow, TET, etc.), among others. It implies that a fuel-optimized trajectory represents in fact a tradeoff among all these parameters, some of which conflict with each other.

The flight profile optimized for minimum  $\text{NO}_x$  emissions is flown similar to the fuel-optimized one, i.e., mostly slower (Fig. 5c) and higher (Fig. 5b) than the baseline trajectory utilized. In general, the relative lower speed and higher altitude utilized to fly this trajectory lead to a reduction in the thrust required to fly the trajectory segments. These lower thrust requirements are in turn translated into lower engine TET values (Fig. 5), which ultimately result in a reduction in the level of  $\text{NO}_x$  emissions produced (Fig. 5f). Fig. 5e shows, in particular, that from all TET

values, those corresponding to the  $\text{NO}_x$  emissions, optimised trajectory values are the lowest ones. This is expected, of course, because this parameter has a direct influence on the level of  $\text{NO}_x$  emissions produced. In Fig. 5f, it can also be observed that the changes in  $\text{CO}_2$  and  $\text{H}_2\text{O}$  present the expected behavior, and, even though the  $\text{NO}_x$  emissions optimized trajectory increases the total flight time, the total amount of fuel burned is largely reduced. This is a consequence of the lower engine thrust settings utilized to fly this trajectory. As in the first two case studies, the aircraft trajectory optimized for minimum flight time significantly increases the amount of  $\text{NO}_x$  emissions (Fig. 5f). This is partially due to the large amount of thrust required to fly some of the segments of this particular optimized trajectory.

## CONCLUSIONS

Initial results obtained using optimization algorithms (i.e., Polyphemus) capable of performing multidisciplinary aircraft trajectory optimization processes were described in this work. A short description of both the rationale behind the initial selection of a suitable optimization technique and the status of Polyphemus was firstly presented. The Polyphemus optimizer was subsequently utilized to analyze three different case studies involving the optimization of one or more phases of actual aircraft flight profiles. Results related to optimum trajectories obtained using Polyphemus, minimization of total flight time, fuel burned and  $\text{NO}_x$  emissions were presented and discussed. The results obtained using Polyphemus and other commercially available optimization algorithms presented a satisfactory level of agreement (average discrepancies ~2%). Further developments on Polyphemus are currently underway in order to identify and efficiently compute optimum and 'greener' aircraft trajectories, which help minimize the impact of commercial aircraft operations on the environment. It is worth emphasizing that the main objective of different case studies analyzed was the evaluation of the mathematical performance of Polyphemus rather than the generation of realistic aircraft trajectories. As, in general, these different case studies provided mathematically and conceptually correct solutions, it is concluded that the approach utilized in this work for carrying out the aircraft trajectory optimization processes is a valid one. This, of course, provides the necessary motivation for continuing with the development of the Polyphemus optimizer.



## ACKNOWLEDGMENTS

During this work, Cesar Celis was partially supported by the Programme Alβan, the European Union Programme of High Level Scholarships for Latin America, Scholarship No. E07D400097BR. Source of financing: European Union.

The authors would like to extend their gratitude to both Mr. Hasan Zolata, who using commercially available algorithms produced some of the results mention here, and Dr. Jean-Michel Rogero, whose PhD research at CU has provided a foundation for the Polyphemus optimizer used in this work. Special thanks also to Mr. Richard Long, who developed the aircraft performance model utilized.

## REFERENCES

- Betts, J., 1998, "Survey of Numerical Methods for Trajectory Optimization", *Journal of Guidance, Control, and Dynamics*, Vol. 21, No. 2, pp. 193–207.
- Boeing Commercial Airplanes, "Market Analysis, Boeing Current Market Outlook 2009 to 2028", Available from: [www.boeing.com/cmo](http://www.boeing.com/cmo). Accessed on: 16 August 2009.
- Brooker, P., 2006, "Civil Aircraft Design Priorities: Air Quality? Climate Change? Noise?", *The Aeronautical Journal*, Vol. 110, No. 1110, pp. 517–532.
- Bunday, B.D., 1984, "Basic Optimisation Methods", Edward Arnold, London, UK.
- Callan, R., 2003, "Artificial Intelligence", Palgrave Macmillan, New York, US.
- Celis, C., 2010, "Evaluation and Optimisation of Environmentally Friendly Aircraft Propulsion Systems", Ph.D. Thesis, School of Engineering, Cranfield University.
- Celis, C., Long, R., Sethi, V. and Zammit-Mangion, D., 2009, "On Trajectory Optimisation for Reducing the Impact of Commercial Aircraft Operations on the Environment", 19th Conference of the International Society for Air Breathing Engines, ISABE-2009, Montréal, Canada.
- Celis, C., Moss, B. and Pilidis, P., 2009, "Emissions Modelling for the Optimisation of Greener Aircraft Operations", *Proceedings of GT2009, ASME Turbo Expo 2009, Power for Land, Sea and Air*, Orlando, Florida, USA.
- Clarke, J.P., 2003, "The Role of Advanced Air Traffic Management in Reducing the Impact of Aircraft Noise and Enabling Aviation Growth", *Journal of Air Transport Management*, Vol. 9, No. 3, pp. 161–165.
- Clean Sky JTI (Joint Technology Initiative), 2009, Available from: [www.cleansky.eu](http://www.cleansky.eu). Accessed on: 18 August 2009.
- Davis, L. (editor), 1991, "Handbook of Genetic Algorithms", Van Nostrand Reinhold, New York, US.
- Everitt, B., 1987, "Introduction to Optimization Methods and their Application in Statistics", Chapman and Hall, London, UK.
- Fletcher, R., 1987, "Practical Methods of Optimization", 2nd Edition, John Wiley, Chichester, UK.
- Goldberg, D.E., 1989, "Genetic Algorithms in Search, Optimization and Machine Learning", Addison-Wesley, Reading, MA, US.
- Green, J. E., 2003, "Civil Aviation and the Environmental Challenge", *The Aeronautical Journal*, Vol. 107, No. 1072, pp. 281–299.
- Gulati, A., 2001, "An Optimization Tool for Gas Turbine Engine Diagnostics", Ph.D. Thesis, School of Engineering, Cranfield University.
- Hartley, S.J., 1998, "Concurrent Programming: The Java Programming Language", Oxford University Press, New York, US.
- Krotov, V.F., 1996, "Global Methods in Optimal Control Theory", Marcel Dekker, New York, US.
- Long, R.F., 2009, "An Aircraft Performance Model for Trajectory Optimisation", School of Engineering, Cranfield University, UK (unpublished).
- MATLAB®, 2008, "The Language of Technical Computing, Version 7.7 (R2008b)", The MathWorks, Inc. Available from: [www.mathworks.com](http://www.mathworks.com).
- Palmer, J.R., 1999, "The TurboMatch Scheme for Gas-Turbine Performance Calculations, User's Guide", Cranfield University, Cranfield, UK.
- PARTNER, 2009, "Partnership for Air Transportation Noise and Emissions Reduction", Available from: [web.mit.edu/aeroastro/partner/](http://web.mit.edu/aeroastro/partner/). Accessed on: 18 August 2009.
- Quagliarella, D., 1998, "Genetic Algorithms and Evolution Strategy in Engineering and Computer Science, Recent Advances and Industrial Applications", John Wiley & Sons, Ltd., Chichester, UK.
- Rao, S.S., 1996, "Engineering Optimization: Theory and Practice", 3rd Edition, John Wiley, New York, US.
- Riddlebaugh, S.M. (editor), 2007, "Research & Technology 2006, NASA/TM – 2007-214479", NASA Glenn Research Center, Cleveland, Ohio, USA.
- Rogero, J.M., 2002, "A Genetic Algorithms-based Optimisation Tool for the Preliminary Design of Gas Turbine Combustors", Ph.D. Thesis, School of Mechanical Engineering, Cranfield University.
- Rogero, J.M. and Rubini, P.A., 2003, "Optimisation of Combustor Wall Heat Transfer and Pollutant Emissions for Preliminary Design Using Evolutionary Techniques", *Proceedings of the Institution of Mechanical Engineers, Part A: Journal of Power and Energy*, Vol. 217, No. 6, pp. 605–614.
- Russell, S. and Norvig, P., 2003, "Artificial Intelligence: A Modern Approach", 2nd Edition, Prentice Hall, New Jersey, US.
- Sampath, S., 2003, "Fault Diagnostics for Advanced Cycle Marine Gas Turbine Using Genetic Algorithms", Ph.D. Thesis, School of Engineering, Cranfield University.
- Schwefel, H.P., 1981, "Numerical Optimization of Computer Models", John Wiley, Chichester, UK.
- Walsh, G.R., 1975, "Methods of Optimization", John Wiley, London, UK.
- Wienke, D., Lucasius, C.B. and Kateman, G., 1992, "Multicriteria Target Vector Optimization of Analytical Procedures Using a Genetic Algorithm. Part I. Theory, Numerical Simulation and Application to Atomic Emission Spectroscopy", *Analytica Chimica Acta*, Vol. 265, No. 2, pp. 211–225.

2014-03-01

# Theoretical optimal trajectories for reducing the environmental impact of commercial aircraft operations

Celis, Cesar

Institute of Aeronautics and Space

---

Celis C, Sethi V, Zammit-Mangion D, et al., (2014) Theoretical optimal trajectories for reducing the environmental impact of commercial aircraft operations. *Journal of Aerospace Technology and Management*, Volume 6, Issue 1, January-March 2014, pp. 29-42

<https://doi.org/10.5028/jatm.v6i1.288>

*Downloaded from Cranfield Library Services E-Repository*